JOURNAL OF THEORETICAL AND APPLIED MECHANICS
42, 1, pp. 69-82, Warsaw 2004

A NON-LOCAL FATIGUE CRACK GROWTH MODEL AND ITS EXPERIMENTAL VERIFICATION[1]

Andrzej Seweryn
Adam Tomczyk

Faculty of Mechanical Engineering, Białystok University of Technology
e-mail: seweryn@pb.bialystok.pl

Zenon Mróz

Institute of Fundamental Technological Research, Polish Academy of Sciences, Warsaw
e-mail: zmroz@ippt.gov.pl

The present paper is concerned with the modelling of fatigue crack initiation and propagation by applying the non-local critical plane model, proposed by Seweryn and Mróz (1996, 1998). Using the linear elastic stress field at the front of a crack or sharp notch, the damage growth on a physical plane is specified in terms of mean values of the stress and strength function. The model is applied to study crack propagation under cyclically varying tension-compression conditions. The predictions are compared with experimental data.

Key words: fatigue, damage accumulation, crack propagation

1. Introduction

Most engineering elements subjected to variable loads experience multiaxial stress and strain states for which the principal stress vary in time. Usually, the elements contain stress concentrators (notches, holes, joints), which amplify nominal stresses and generate fatigue cracks. In most cases of combined loads the notch tip stress and strain fields do not vary proportionally, and multiaxial fatigue parameters should be introduced to provide crack initiation and propagation conditions. Most fatigue data in the form of S-N curves have

[1]This paper was presented on *Symposium Damage Mechanics of Materials and Structures*, June 2003, Augustów, Poland, 2003

been generated for uniform specimens under uniaxial loading and next used to predict the fatigue life for notched specimens in terms of the local stress and strain amplitudes.

The critical plane approaches have been widely used in correlating fatigue data and in formulating fatigue conditions. This approach is natural since the plane crack initiation and growth is dependent on the surface traction components, and the resulting crack opening and shear provide damage strains associated with the crack surface.

Consider a physical plane in a material element specified by the unit normal vector $\boldsymbol{n}$. The plane traction vector and its components are

$$\boldsymbol{T} = \boldsymbol{\sigma n} \qquad \sigma_n = (\boldsymbol{n} \cdot \boldsymbol{\sigma n})\boldsymbol{n} \qquad \boldsymbol{\tau}_n = (\mathbf{I} - \boldsymbol{n} \otimes \boldsymbol{n})\boldsymbol{\sigma n} \tag{1.1}$$

Similarly, the surface strain components are

$$\boldsymbol{\Gamma} = \boldsymbol{\varepsilon n} \qquad \varepsilon_n = (\boldsymbol{n} \cdot \boldsymbol{\varepsilon n})\boldsymbol{n} \qquad \boldsymbol{\gamma}_n = (\mathbf{I} - \boldsymbol{n} \otimes \boldsymbol{n})\boldsymbol{\varepsilon n} \tag{1.2}$$

where $\mathbf{I}$ is the identity tensor. The critical plane can be assumed in advance as a representative plane on which the critical condition is satisfied. It was first Findley *et al.* (1956) was the first to postulate that the representative plane is the maximum shear plane with both shear and normal strain amplitudes specifying the damage parameter. A particular form of the mentioned condition was proposed by Brown and Miller (1973). McDiarmid (1991) provided an alternative stress condition expressing the fatigue parameter in terms of shear and normal stress amplitudes on the maximal shear planes. Other criteria of this type combine the shear strain amplitude and the maximal normal stress acting on the maximal shear plane, cf. Socie (1993).

These conditions can be easily applied to the case of proportional loading. However, for non-proportional loading, the proper definition of stress and strain amplitudes should be generated. Furthermore, experimental observations indicate that cracks do not develop on the maximum shear planes for all metals.

A more consistent approach is not obtained by specifying the critical plane approach in advance but requiring the maximum of the failure condition to be reached with respect to all orientations, thus

$$\max_{\boldsymbol{n}} F(\sigma_n, \tau_n, \varepsilon_n, \gamma_n) = F_c \tag{1.3}$$

where F_c represents the critical value reached by the failure condition. The present definition provides the critical plane which is also the extremal plane, so that the critical condition is not violated on other potential failure planes.

A particular form of Eq. (1.3) is obtained by applying the strain energy density associated with the amplitudes of stress and strain components acting on the critical plane, cf. Glinka *et al.* (1995). This parameter represents only a fraction of the strain energy. However, it does not account for the effect of the mean stress. An alternative energy condition was proposed by Chu (1995) by combining the maximum normal and shear stresses with the strain amplitudes. The formulation of Seweryn and Mróz (1996, 1998) followed the idea of the non-local stress or strain measures on the critical plane area of size $d_0 \times d_0$. In the present paper, we shall develop this critical plane model for the prediction of fatigue crack propagation under uniaxial loading conditions. The predictions are compared with experimental data.

2. Basic assumptions

To illustrate applicability of the model, consider a plate of uniform thickness (Fig. 1a) with an edge crack of the length l, loaded by a cyclically varying stress σ of the amplitude $\Delta\sigma$ and mean value $\sigma_m = \Delta\sigma/2$ (Mróz *et al.*, 2000). The material is assumed to be linear elastic but exhibiting a process or damage zone Ω of the length d_0 at the crack tip (Fig. 1b).

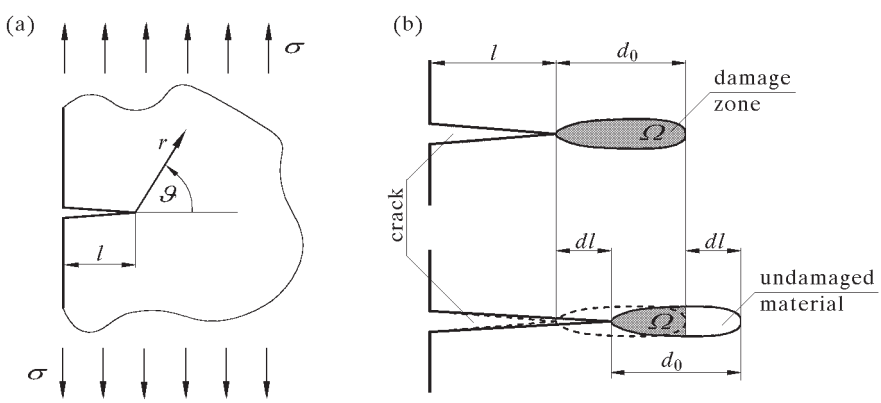

Fig. 1. (a) Polar coordinate system connected with the tip of the edge crack, (b) scheme of the damage zone propagation

The existence of the localized damage zone is usually assumed for the cohesive crack model with an additional rule relating the stress to displacement discontinuity. Here, however, the stress distribution will be treated within the

linear elasticity but the existence of the process zone will be accounted for using the non-local damage rule discussed in the previous section.

It is assumed that damage growth occurs only in the damage zone and is specified by the mean value $\overline{\omega}_n$ affecting the critical stress σ_c. The mean value of the normal stress in the zone Ω equals

$$\overline{\sigma}_n = \frac{1}{d_0}\int_0^{d_0} \sigma_n \, dr = \frac{2K_{\mathrm{I}}}{\sqrt{2\pi d_0}} \tag{2.1}$$

where K_{I} is the stress intensity factor for mode I. Let us note that $\overline{\sigma}_n$ is twice as large as the stress value at the end of the damage zone.

3. Damage accumulation and crack growth in one cycle of loading

We divide the cycle of fatigue loading into four stages (Fig. 2).

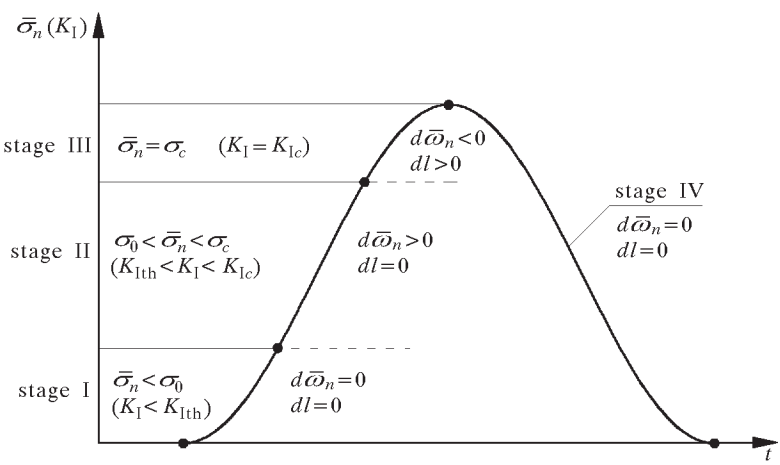

Fig. 2. Consecutive stages in one loading cycle

When the stress in a cycle increases from zero, then in stage I there is no damage growth as $\overline{\sigma}_n < \sigma_0$ and $K_{\mathrm{I}} < K_{\mathrm{Ith}}$ where σ_0, and K_{Ith} are the damage initiation threshold values. Let us note that both σ_0 and K_{Ith} depend on the damage state, thus

$$\sigma_0 = \sigma_0^*(1-\overline{\omega}_n)^p \qquad K_{\mathrm{Ith}} = K_{\mathrm{Ith}}^*(1-\overline{\omega}_n)^p \tag{3.1}$$

where σ_0^* and K_{Ith}^* are the respective values for the undamaged material.

In the second stage $\sigma_0 < \overline{\sigma}_n < \sigma_c$, the damage growth occurs in the zone Ω, according to the following rule

$$d\overline{\omega}_n = A\Big(\frac{\overline{\sigma}_n - \sigma_0}{\sigma_c - \sigma_0}\Big)^n \frac{d\overline{\sigma}_n}{\sigma_c^* - \sigma_0^*} \qquad d\overline{\sigma}_n > 0 \qquad \overline{\sigma}_n > \sigma_0 \tag{3.2}$$

and we have

$$\sigma_c = \sigma_c^*(1-\overline{\omega}_n)^p \qquad K_{\mathrm{I}c} = K_{\mathrm{I}c}^*(1-\overline{\omega}_n)^p \tag{3.3}$$

where σ_c^* and $K_{\mathrm{I}c}^*$ are the critical values for the undamaged material.

Let us note that in Eq. (3.2) the stress difference $(\sigma_c^* - \sigma_0^*)$ in the denominator occurs. This differs from the original formulation of Seweryn and Mróz (1996) where the form $(\sigma_c - \sigma_0)$ was used. Introduce the ratio $\sigma_0^*/\sigma_c^* = \eta$ and assume that

$$\eta = \frac{\sigma_0^*}{\sigma_c^*} = \frac{\sigma_0}{\sigma_c} = \frac{K_{\mathrm{Ith}}}{K_{\mathrm{I}c}} = \frac{K_{\mathrm{Ith}}^*}{K_{\mathrm{I}c}^*} \tag{3.4}$$

In view of Eqs (3.1), (3.3) and (3.4), the damage evolution rule takes the form

$$d\overline{\omega}_n = \frac{A}{(1-\eta)^{n+1}}\Big(\frac{K_{\mathrm{I}}}{K_{\mathrm{I}c}^*(1-\overline{\omega}_n)^p} - \eta\Big)^n \frac{dK_{\mathrm{I}}}{K_{\mathrm{I}c}^*} \tag{3.5}$$

A this stage, the stress value $\overline{\sigma}_n$ increases but the values of σ_0 and σ_c decrease, according to Eqs (3.1) and (3.3). When $\overline{\sigma}_n$ reaches the critical value $\overline{\sigma}_n = \sigma_c$ and $K_{\mathrm{I}} = K_{\mathrm{I}c}$, the crack growth process occurs, so that the condition

$$\begin{aligned} &F_c = \overline{\sigma}_n - \sigma_c = \overline{\sigma}_n - \sigma_c^*(1-\overline{\omega}_n)^p = 0 \qquad \text{or} \\ &\overline{F}_c = K_{\mathrm{I}} - K_{\mathrm{I}c} = K_{\mathrm{I}} - K_{\mathrm{I}c}^*(1-\overline{\omega}_n)^p = 0 \qquad \text{and} \qquad dl > 0 \end{aligned} \tag{3.6}$$

is satisfied.

The consistency condition for the growth crack is

$$dF_c = d\overline{\sigma}_n - d\sigma_c = 0 \qquad d\overline{F}_c = dK_{\mathrm{I}} - dK_{\mathrm{I}c}(\overline{\omega}_n) = 0 \tag{3.7}$$

Let us note that $K_{\mathrm{I}} = K_{\mathrm{I}}(\sigma, l)$, so we have

$$dK_{\mathrm{I}} = \frac{\partial K_{\mathrm{I}}}{\partial \sigma} d\sigma + \frac{\partial K_{\mathrm{I}}}{\partial l} dl \tag{3.8}$$

In most cases, the first term dominates as the crack growth value dl/dN is small. Then

$$dK_{\mathrm{I}} \cong M_k \sqrt{\pi l}\; d\sigma \tag{3.9}$$

where M_k depends on the geometry of the plate.

The damage growth during the propagation stage is decomposed into two terms

$$d\overline{\omega}_n = d\overline{\omega}_{n1} + d\overline{\omega}_{n2} \qquad d\overline{\omega}_{n1} > 0 \qquad d\overline{\omega}_{n2} < 0 \tag{3.10}$$

where the first term is associated with the loading increment and the second is associated with the damage zone propagation, so

$$\begin{aligned} d\overline{\omega}_n &= \frac{2AdK_{\mathrm{I}}}{\sqrt{2\pi d_0}(\sigma_c^* - \sigma_0^*)} - \overline{\omega}_n \frac{dl}{d_0} \qquad \text{or} \\ \frac{dl}{d_0} &= -\Big[1 + \frac{pA}{(1-\eta)}(1-\overline{\omega}_n)^{p-1}\Big]\frac{d\overline{\omega}_n}{\overline{\omega}_n} \end{aligned} \tag{3.11}$$

Integrating Eq. (3.11), we obtain

$$\frac{\Delta l}{d_0} = -\int_{\overline{\omega}_{nk}}^{\overline{\omega}_{np}} \Big[1 + \frac{pA}{(1-\eta)}(1-\overline{\omega}_n)^{p-1}\Big]\frac{d\overline{\omega}_n}{\overline{\omega}_n} \tag{3.12}$$

where $\overline{\omega}_{nk}$ and $\overline{\omega}_{np}$ denote the damage values at the beginning and the end of propagation stage III. Noting that

$$K_{\mathrm{I}}^* = K_{\mathrm{I}c}^*(1-\overline{\omega}_{nk})^p \qquad K_{\mathrm{I}max} = K_{\mathrm{I}c}^*(1-\overline{\omega}_{np})^p \tag{3.13}$$

where K_{I}^* denotes the stress intensity factor at the beginning of the propagation stage, relation (3.12) can be rewritten in the form

$$\frac{\Delta l}{d_0} = \frac{1}{p}\int_{K_{\mathrm{I}}^*}^{K_{\mathrm{I}max}} \Big[\frac{C(K_{\mathrm{I}})^{\left(\frac{1}{p}-1\right)} + BC^p}{1 - C(K_{\mathrm{I}})^{\frac{1}{p}}}\Big]\, dK_{\mathrm{I}} \tag{3.14}$$

where

$$C = \Big(\frac{2}{\sigma_c^*\sqrt{2\pi d_0}}\Big)^{\frac{1}{p}} \qquad B = \frac{pA}{1-\eta}$$

Relations (3.12) and (3.14) specify the crack growth during one cycle, so that $\Delta l = dl/dN$. Consecutive stage IV corresponds to elastic unloading, so that

$$d\overline{\sigma}_n < 0 \qquad dK_{\mathrm{I}} < 0 \qquad d\overline{\omega}_n = 0 \qquad dl = 0 \tag{3.15}$$

Using the double logarithmic scale, the crack propagation curves are shown in Fig. 3, for varying exponents n and for varying values of the damage

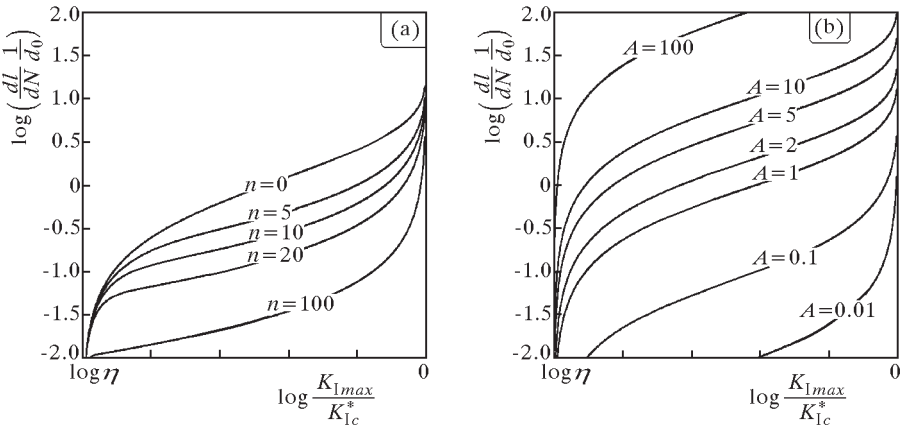

Fig. 3. Crack propagation curves $\log(\Delta l/d_0)$ versus $\log(K_{Imax}/K^*_{Ic})$: (a) dependence on the exponent n, (b) dependence on the parameter A

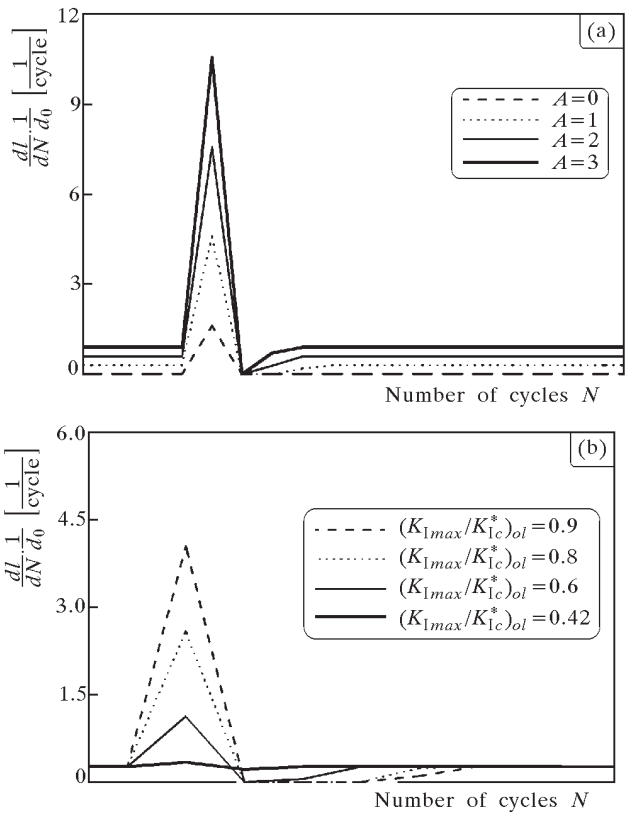

Fig. 4. The effect of a single overloading cycle on crack propagation rates: (a) single overloading cycle $K_{Imax}/K^*_{Ic}=0.9$ and subsequent cycles $K_{Imax}/K^*_{Ic}=0.5$; (b) single overloading cycle $K_{Imax}/K^*_{Ic}=0.42$, 0.6, 0.8, 0.9 with subsequent cycles $K_{Imax}/K^*_{Ic}=0.4$

growth parameter A. The curves can be compared with the usual diagrams $dl/dN = f(\Delta K_{\mathrm{I}})$ available in literature. It is seen that the crack propagation curves correspond qualitatively well to experimental curves. When K_{I} tends to K^*_{Ic}, the crack propagation rate tends to infinity, when K_{I} tends to K_{Ith}, the propagation rate tends to zero (or the logarithmic measure to minus infinity).

Figure 4 illustrate the effect of overloading on the subsequent crack propagation rate for a single overloading cycle and different values of A and overloading amplitude.

The model presented in this section considers the translation of the damage zone at the propagating crack tip. It is possible to propose an alternative approach considering both: motion of the damage zone and growth of this zone.

4. Unstable crack growth condition

Let us note that when K_{I} tends to K^*_{Ic} (or $\overline{\sigma}_n$ tends to σ^*_c), then the case of brittle fracture occurs. Let us remind that the first term of Eq. (3.8) dominates for the stable crack growth, and the second term is greater for the unstable growth. To formulate the brittle fracture condition, we can disregard the first term of Eq. (3.8) because

$$\frac{\partial K_{\mathrm{I}}}{\partial \sigma} d\sigma \ll \frac{\partial K_{\mathrm{I}}}{\partial l} dl \qquad \text{so} \qquad dK_{\mathrm{I}} \approx \frac{\partial K_{\mathrm{I}}}{\partial l} dl \tag{4.1}$$

which is justified in the case of the load control (then $d\sigma/dl \geqslant 0$). When a kinematic control occurs, we have $d\sigma/dl < 0$ and it is necessary to consider the complete form of (3.8).

Rearranging Eq. (3.7), we can formulate the brittle fracture criterion in the following form:

— crack propagation condition

$$K_{\mathrm{I}} = K^*_{\mathrm{Ic}}(1 - \overline{\omega}_n)^p \tag{4.2}$$

— unstable crack growth condition

$$\frac{\partial K_{\mathrm{I}}}{\partial l} \geqslant \frac{pK^*_{\mathrm{Ic}}(1 - \overline{\omega}_n)^p \overline{\omega}_n}{d_0\Big[1 - \overline{\omega}_n + \frac{pA}{1-\eta}(1 - \overline{\omega}_n)^p\Big]} \tag{4.3}$$

An alternative form of (4.3) is

$$\frac{\partial K_{\mathrm{I}}}{\partial l} \geqslant \frac{K_{\mathrm{I}}}{d_0} \frac{p\left[1-\left(\frac{K_{\mathrm{I}}}{K^*_{\mathrm{Ic}}}\right)^{\frac{1}{p}}\right]}{\left(\frac{K_{\mathrm{I}}}{K^*_{\mathrm{Ic}}}\right)^{\frac{1}{p}} + \frac{pA}{1-\eta}\frac{K_{\mathrm{I}}}{K^*_{\mathrm{Ic}}}} \tag{4.4}$$

Figure 5 shows a graphic illustration of these equations.

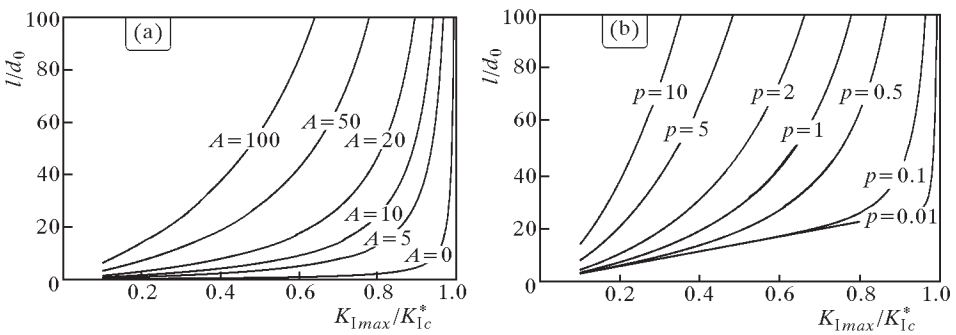

Fig. 5. Dependence of the critical crack length on K_{I} for the unstable crack growth (a) $p = 1$, $\eta = 0.1$, (b) $A = 50$, $\eta = 0.1$

5. Experimental verification

An experimental program was executed by plane testing specimens of PMMA with edge notches. The selection of the material was motivated by its linear elastic response and the possibility of visual observation of the crack tip. The tests were carried out using the MTS tensile machine, and the crack growth measurement was realised by means of a spiral microscope (VEB Carl Zeiss Jena) with accuracy of the order of 0.001 mm. Fig. 6 and Fig. 7 present the experimental data of the crack growth measurement and the predicted values pertaining to the present model. The comparison with the prediction resulting from Paris (1963) equation

$$\frac{dl}{dN} = C(\Delta K)^m \tag{5.1}$$

was also presented.

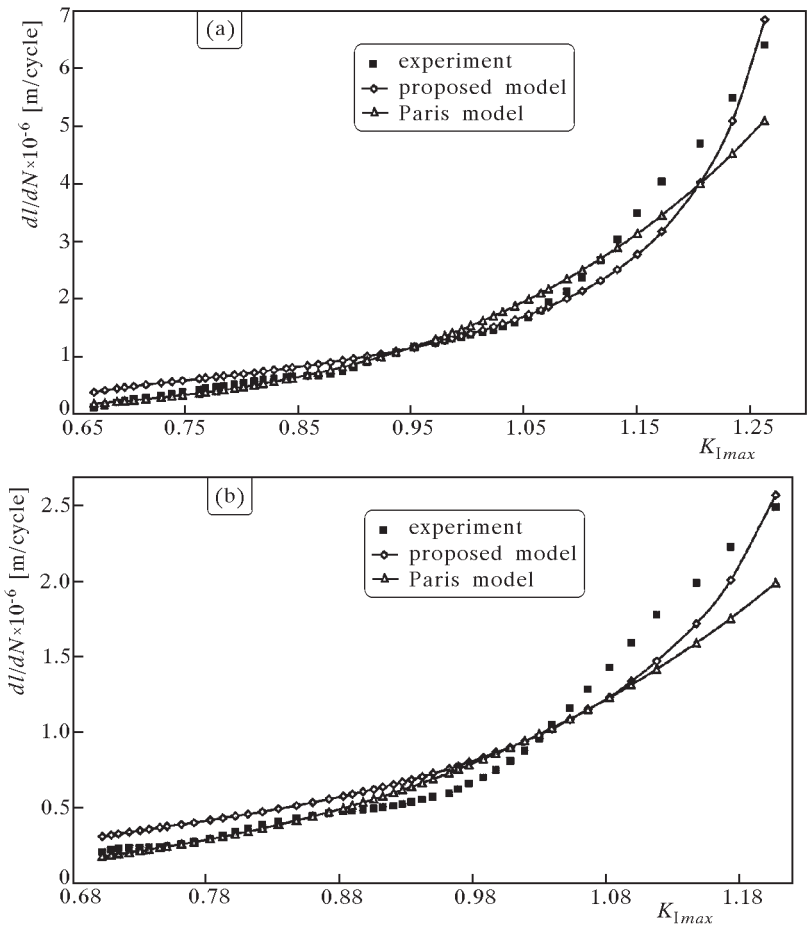

Fig. 6. Diagrams of fatigue crack growth: comparison of experimental data with model prediction: (a) specimen 14A, (b) specimen 14B

Five types of specimens were used $(12A, 12B, 12C, 14A, 14B)$ in the tests. The parameter specification for the Paris model is presented in Table 1, and of the present model in Table 2.

It is seen that the parameter values are scattered, which typical for fatigue tests for PMMA. The present model predicts much better fatigue crack growth, especially for high values of $K_{\mathrm{I}max}$ close to $K^*_{\mathrm{I}c}$. We note that the value of the parameter p equals one, and then the specification of damage zone growth is essentially simplified. It is also interesting to note that the maximum size of the damage zone $d_0 = 0.16\,\mathrm{mm}$ was confirmed from both static and cyclic

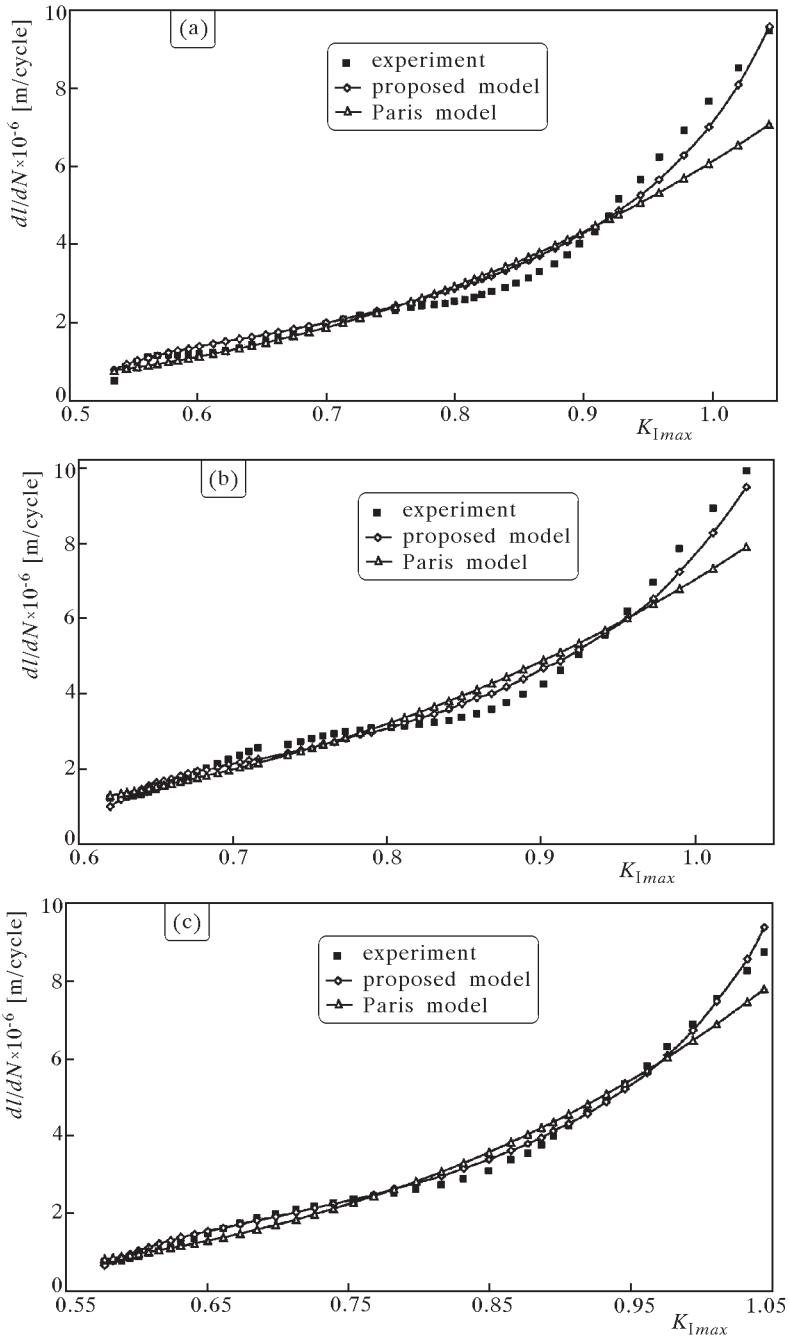

Fig. 7. Diagrams of fatigue crack growth: comparison of experimental data with model prediction: (a) specimen 12A, (b) specimen 12B, (c) specimen 12C

loading tests, providing good correlation with the experimental data. Biaxial stress programs are being currently tested, and the prediction of crack paths will be compared with measurements.

Table 1. Parameter specification for Paris equation

Sample No.	C	m
$12A$	6.19×10^{-7}	3.31
$12B$	7.09×10^{-7}	3.55
$12C$	6.65×10^{-7}	3.78
$14A$	1.52×10^{-6}	5.21
$14B$	8.66×10^{-7}	4.43

Table 2. Parameter specification for present model

Sample No.	A	n	p	K^*_{Ith} [MPa$\sqrt{\mathrm{m}}$]	K^*_{Ic} [MPa$\sqrt{\mathrm{m}}$]	d_0 [mm]
$12A$	0.009	9	1	0.5	1.2	0.16
$12B$	0.013	12.5		0.6	1.2	
$12C$	0.007	7		0.55	1.2	
$14A$	0.024	7		0.6	1.35	
$14B$	0.017	8		0.6	1.35	

Unstable crack growth condition (4.4) for loading mode I was also verified. Let us remind that for each sample, the parameter p equals 0, so equation (4.4) can be rewritten in the form

$$\frac{\partial K_{\mathrm{I}}}{\partial l} \geqslant \frac{K_{\mathrm{I}}}{d_0} \frac{1 - \frac{K_{\mathrm{I}}}{K^*_{\mathrm{Ic}}}}{\frac{K_{\mathrm{I}}}{K^*_{\mathrm{Ic}}}\left(1 + \frac{A}{1-\eta}\right)} \tag{5.2}$$

To verify the unstable crack growth condition, the critical values l_c were calculated according to equation (5.2) and presented in Table 3. The values $l_{c\,exp}$ were measured after experimental tests from the surface of fatigue fractures. It is possible that the values l_c are a little underrated because it was assumed that the decohesion process occurs when $K_{\mathrm{I}} = K_{\mathrm{I}max}$. In reality, a crack could start propagate unstable in the last cycle of the loading for $K_{\mathrm{I}} < K_{\mathrm{I}max}$ – which corresponds with a greater value of the damage measure $\overline{\omega}_n$.

Table 3. Critical values of the crack length and corresponding values $\partial K_{\mathrm{I}}/\partial l$

Sample No.	$\frac{\partial K_{\mathrm{I}}}{\partial l}\left[\frac{\mathrm{MPa}}{\sqrt{\mathrm{m}}}\right]$	$l_{c\,exp}$ [mm]	l_c [mm]
$12A$	51.949	12.63	14.588
$12B$	51.943	13.19	14.587
$12C$	51.948	13.33	14.589
$14A$	59.317	13.17	13.757
$14B$	59.320	13.22	13.754

6. Concluding remarks

The present paper provides a model for the analysis of crack initiation and propagation for monotone and variable loadings. A damage zone of a constant length is introduced with averaged measures of the stress and damage within the zone. The zone is assumed to propagate with the crack tip when the critical propagation condition is reached. Stable and unstable growth stages can be treated.

The model proposed enables calculation of the crack growth in a linear elastic material and analysis of the effect of overloads on the crack growth rate. The analysis is confined to asymptotic stress fields near the crack tip. However, it can be extended to more complex descriptions containing more terms of asymptotic expansions or generated by approximate methods. The analysis can also be extended to two dimensional stress states and the associated damage zones. Furthemore the damage initiation function and the stress failure function can be then introduced to describe damage accumulation and crack propagation processes in a cycle of the loading.

Acknowledgement

The investigation described in this paper is a part of the research project No. 8 T07A 049 21 sponsored by the State Committee for Scientific Research.

References

1. Brown M.W., Miller K.J., 1973, A theory for fatigue failure under multiaxial stress-strain conditions, *Proc. of the Institute of Mechanical Engineers*, **187**, 745-755

2. CHU C.C., 1995, Fatigue damage calculation using the critical plane approach, *J. Engng Mat. Techn.*, **117**, 41-49

3. FINDLEY W.N., COLEMAN J.J., HANDLEY B.C., 1956, Theory for combined bending and torsion fatigue data for 4340 steel, *Proc. Int. Conf. Fatigue of Metals*, The Inst. Mech. Eng., 150-157

4. GLINKA G., SHEN G., PLUMTREE A., 1995, A multiaxial fatigue strain energy density parameter related to the critical plane, *Fatigue and Fract. Engng Mat. Struct.*, **18**, 37-46

5. MCDIARMID D.L., 1991, A general criterion for high-cycle multiaxial fatigue failure, *Fatigue Fract. Engng Mater. Struct.*, **14**, 429-453

6. MORROW J., 1965, Cyclic plastic strain energy and fatigue of metals, *Internal Friction Damping and Cyclic Plasticity*, ASTM STP, **378**, 45-87

7. MRÓZ Z., SEWERYN A., TOMCZYK A., 2000, A non-local critical plane model for the analysis of fatigue crack propagation, In: *Continuous Damage and Fracture*, Ed. Benallal A., Elsevier, 373-384

8. PARIS P., ERDOGAN F., 1963, A critical analysis of crack propagation laws, *J. Basic Engng, Trans. ASME*, 528-534

9. SEWERYN A., MRÓZ Z., 1996, A non-local stress failure and fatigue damage accumulation condition, In: *Multiaxial Fatigue and Design*, Eds: Pineau A., Cailletaud G., Lindley T.C., 259-280, Mech. Eng. Publ., London

10. SEWERYN A., MRÓZ Z., 1998, On the criterion of damage evolution for variable multiaxial stress state, *Int. J. Solids and Struct.*, **35**, 1599-1616

11. SOCIE D.F., 1993, Critical plane approaches for multiaxial fatigue damage assessment, *Advances in Mechanical Fatigue*, ASTM STP, **119**, 7-36

Nieokalny model wzrostu szczeliny zmęczeniowej i jego doświadczalna weryfikacja

Streszczenie

Praca dotyczy modelowania inicjacji i propagacji szczeliny zmęczeniowej przy wykorzystaniu nielokalnego podejścia związanego z płaszczyzną krytyczną (Seweryn i Mróz, 1996, 1998). Wykorzystując liniowo sprężyste pola naprężeń przed wierzchołkiem szczeliny opisano kumulację uszkodzeń i wzrost szczeliny na płaszczyźnie fizycznej. Do rozważań przyjęto uśrednioną w strefie kumulacji uszkodzeń miarę uszkodzeń oraz uśrednione naprężenia. Wyniki obliczeń numerycznych porównano z wynikami badań doświadczalnych.

Manuscript received October 1, 2003; accepted for print October 20, 2003